

Field-theoretical approach to a dense polymer with an ideal binary mixture of clustering centers

Riccardo Fantoni*

National Institute for Theoretical Physics (NITheP) and Institute of Theoretical Physics, Stellenbosch 7600, South Africa

Kristian K. Müller-Nedebock†

*Institute of Theoretical Physics, Department of Physics,
Stellenbosch University, Private Bag X1, Matieland 7602, South Africa*

(Dated: July 1, 2011)

We propose a field-theoretical approach to a polymer system immersed in an ideal mixture of clustering centers. The system contains several species of these clustering centers with different functionality, each of which connects a fixed number segments of the chain to each other. The field-theory is solved using the saddle point approximation and evaluated for dense polymer melts using the Random Phase Approximation. We find a short-ranged effective inter-segment interaction with strength dependent on the average segment density and discuss the structure factor within this approximation. We also determine the fractions of linkers of the different functionalities.

PACS numbers: 61.41.+e,61.25.hp,61.25.he,61.25.H-

Keywords: Field-theory, polymers, clustering, Janus particles.

I. INTRODUCTION

In this work we consider a system where a single polymer chain is immersed in an ideal binary mixture of clustering centers. The study of the resulting associating polymers has a long history (see, e.g., in [1, 2] and references in them). Models for the reversible gelation of polymers range from the consideration of pairwise associations of sticky chain segments [3] to the formation of arbitrary size clusters due to association of dipolar elements in polymer chains [4]. Whereas a large number of theoretical treatments model association with some form of crosslinking, i.e. linking of two segments only, or arbitrary size clusters, we present a treatment for a small number of species of clusters consisting of a fixed number of polymer segments. This falls into the so-called closed multimerization scenario [5].

The reversible or permanent linking of polymer chains or sections of polymers has been a topic of extensive investigations for many decades in a wide range of systems. The general statistical physical scenario generally requires evaluating both the the statistical physics of the chains within a certain linked scenario as well as a summation over all compatible modes of linking the polymer constituents. Independent of whether the linking (crosslinking, aggregation, clustering, type of polycondensation, etc.) is permanent or reversible the topologically and geometrically permissible combinations of linking or clustering need to be evaluated, albeit with different strategies for quenched or annealed situations [6]. Therefore it is natural to think in terms of the enumeration of graphs, as extensively reviewed by Kuchanov, et al. [7]. The ideas can then be applied to a variety of systems, such as associating telechelics [8], polycondensation [9], polymers with multiply aggregating groups [10] and general thermally reversible aggregation, clustering or association [11–19].

There are different possibilities in which the scenario of fixed functionality clustering can be realized. One can think of the segments of the chain connected to particles or sidechains that assemble into structures with closed shells, akin to Janus particles, where it was recently shown that monodisperse ten-particle micelles, and forty-particle vesicles, are the thermodynamically dominant assembled structures [20–22].

We are interested in the properties of a solution of such a polymer with clustering centers and in the relative dominance of co-existing clusters with different, yet fixed, functionalities. To this end we reformulate a field-theoretical method originally proposed by Edwards for permanent, arbitrary-functional end-linking of chains [23]. The resultant field-theory is highly non-linear, but can be treated analytically and numerically, offering an additional theoretical tool to address questions on the formation of localized, reversible structures of polymer chains.

As already mentioned, in order to compute the partition function or free energy one needs to evaluate the polymer chain conformations subject to the restrictions imposed by the functionalities of the linkers and include all possibilities

*Electronic address: rfantoni@ts.infn.it

†Electronic address: kkmn@physics.sun.ac.za

of linking or cluster formation. This is because we are modeling a strong type of aggregation with fixed functionalities, where the clusters are well-defined and local. In other words, all permissible graphs must be generated, their connectivity restrictions be imposed on the polymer chains and weighted appropriately by Boltzmann factors. Kuchanov *et al.* [7], in their exposition of strategies to do this, also point out the very clear analogy between enumeration of spatially embedded graphs and Feynman diagrams from field theories. The obvious utility of a field-theoretical tactic lies in the large spectrum of available approximation techniques and graphical expansions but also in the freedom to choose the precise manner of implementing the additional fields.

In this paper we introduce additional fields, with the associated functional integration, whose role is to produce the desirable linking, network-formation or aggregate possibilities as well as enforcing the spatial consequences of this on the appropriate monomers. The current approach is similar to those used in Refs. [7, 23] and in work that can be seen as precursor to the current formalism [24, 25]. Whereas the specific systems investigated in Refs. [23] and [7] are addressed such that the ends of polymer chains or of star-like polymer units can associate, respectively, the system under investigation here deals with aggregation of segments of a polymer chain. We show that this system allows a formulation of the field theory that has the mathematically advantageous property that it is *local* in the introduced fields and these additional fields also couple to the density of monomers in a local way.

Clearly the sum over aggregated states, by whatever method derived and approximated, would generally impose a complicated form onto the polymer conformational averages. This is also the case for theories with additional fields following integration over the fields. In approximating the functional integral over fields one expects to find nonlinear integral equations for these fields in the kinds of self-consistent field theory calculation that emerge in models for many systems (as in [7, 23]). However, in our formulation the saddle point equations related to the additional fields (and taken before integration over the polymer degrees of freedom) turn out to be only algebraic, albeit nonlinear, providing a significant advantage in tractability in comparison to nonlinear integral equations obtained within other strategies (for other systems). Analysis of the stability, etc. of the resulting theory is also relatively simpler. Completing the integration over the fields incorporates the clustering into the remaining weight for the conformations of the chain (also in a local manner) giving the “structural” contribution that is taken together with the remaining polymer-polymer interactions.

Yet other path integration techniques have made use of generating functional approaches to enumerate tree-like configurations [26–28] in associating systems. Motivated by a wide range of physical scenarios under which polymer chains can aggregate, many different methods (mainly not field-theoretical in the sense as here) have been utilized in determining the contribution of certain classes of connections, ranging from summations over a subset of looped conformations [4], sums of tree-like graphs [29] and trees with cycles to analyses for stickers [3, 8, 30]. Typically the effective polymer-polymer contributions can then be dealt with through a further self-consistent field theory (*e.g.* [31]) or by determining fluctuations with respect to a reference system (*e.g.* [32]) or through a mean-field treatment. In principle, before our approximations at least, the field theory introduced here is not restricted to subsets of connectivities or specifically cyclized conformations nor is it *a priori* a mean-field formalism.

In the current calculation we have a single polymer chain that is immersed in an ideal binary mixture of pointwise clustering centers with different functionality (number of links that the center can have with the polymer segments). As a mathematical device we can think of free segments of the chain being part of clusters of functionality one, *i.e.* they cannot connect to any other segments. Moreover the system is in solution with clustering centers of functionalities a and $b \neq a$. The highly non-Gaussian field-theory resulting from the study of the model is quite complicated but can be approached through the saddle point approximation. Assuming the polymer to be highly dense we can then use the Random Phase Approximation (RPA) to describe the polymer degrees of freedom. We are then able to extract the local densities of segments that form part of clusters of different sizes, the effective potential based on small density fluctuations around a background of a given density, and the static structure factor. In the current treatment we develop the formalism and then investigate properties of the system in the scenario of the uniform polymer segment density with Gaussian fluctuations. However it is also shown where this approximation breaks down. One could certainly expect nonhomogenous phases to develop which can in principle also be addressed by the formalism together with the consideration of higher orders in density fluctuations [33–35].

We shall refer to “polymer segments” as the *monomeric units* of which the polymer chain is built. “Clustering centers” refer to point-like seeds of “clusters” of segments of the polymer chain. In other words the clustering centers function so as to attach to a specific number of the segments of the polymer and in so doing to localise these segments at a common point, binding them reversibly into a cluster. Consequently a polymer segment is also the basic unit to which a single attachment to a single cluster is possible. We shall deal with clustering centers of different functionalities which form a multi-component system with the polymer and provide a “sea” of centers to form clusters with the polymer segments.

Although our field-theoretical formulation includes no precise model for the mechanism that causes clustering centers of a given functionality to occur, we investigate in Section VI the case where the functionalities (10 and 40) of the clustering centers are the same as those determined for Janus particles in recent studies [22]. Indeed there has

recently been much development in the techniques for the synthesis of new patchy colloidal particles [36–39]. One particularly simple class of these anisotropic particles, called Janus particles [40–43], seem to form mainly clusters of either 10 or 40 particles. Here Monte Carlo simulations [20, 21] indicate that mainly stable micelle (10 particles) or vesicle (40 particles) arrangements of these particles are to be found in the vapor phase. Moreover it was found that the clusters behave very similarly to an ideal gas, since the particles forming the cluster tend to arrange with their active surfaces towards the cluster center.

Janus chains have been suggested as potentially useful candidates for understanding interesting polymer phenomena [44]. We will apply our formalism to the case of a dense polymer in a Janus fluid and in so doing we hope to add to the recent interest for Janus particles interacting with polymer chains [43–45]. To the best of our knowledge there are no results in the literature that prove the clustering in the Janus fluid in the presence of the polymer. So we will take as a working hypothesis the existence of such a clustering, and make the approximation of treating the Janus fluid as an ideal mixture of Janus particles, micelles of Janus particles, and vesicles of Janus particles (in the spirit of Ref. [22]).

The paper is organized as follows: in Section II we describe the model we are studying and formulate the field-theory, in Section III we perform the saddle point approximation, and discuss when we expect the approximation to be most accurate. Section IV is devoted to an investigation of dense polymer system with clustering. We use the Random Phase Approximation and derive an expression for the free energy density of the system and the effective interaction caused by the clustering centers. In Section V we determine the structure factor and its curvature at small wave vectors, in Section VI we finally solve the Janus case numerically, and section VII is devoted to the final remarks.

II. THE MODEL

The grand partition function for the ideal binary mixture of clustering centers of functionality a and of functionality b , can be written as

$$\Theta = \sum_{N_1=0}^{\infty} \sum_{N_a=0}^{\infty} \sum_{N_b=0}^{\infty} \frac{(z_1 V)^{N_1}}{N_1!} \frac{(z_a V)^{N_a}}{N_a!} \frac{(z_b V)^{N_b}}{N_b!}$$

where we also allowed for a third species of particles, of functionality one, which cannot cause aggregation. z_i are the usual fugacities for species i , V is the volume of the system, and $N_1 + N_a + N_b$ is the total number of clustering centers.

We now wish to connect these to the polymer degrees of freedom and develop a partition function for the system of polymer together with the clustering centers. The “clusters or clustering centers” represents the free *macro-particles* making up the *ideal mixture* (a two component mixture with clusters of two different functionalities that are living in a “sea” of clusters of functionality one: the *particles*) in which the polymer is immersed. These macro-particles are made up of a fixed number of pointwise *particles* (i.e. they have fixed functionality) each of which is *linked* with one polymer segment.

A suitable field-theoretic formalism was developed by Edwards [23] to describe polymer gels. Consider a field $\phi_1 : \mathbb{R}^3 \rightarrow \mathbb{R}$ then the following Wick’s theorem holds (see Appendix C)

$$\begin{aligned} I(\mathbf{r}_1, \mathbf{r}_2, \dots, \mathbf{r}_{2M}) &= \mathcal{N} \int [d\phi_1] \phi_1(\mathbf{r}_1) \phi_1(\mathbf{r}_2) \dots \phi_1(\mathbf{r}_{2M}) e^{-\frac{1}{2} \int d\mathbf{r} \phi_1^2(\mathbf{r})} \\ &= \sum_{\text{all pairing}} \delta(\mathbf{r}_{l_1} - \mathbf{r}_{l_2}) \delta(\mathbf{r}_{l_3} - \mathbf{r}_{l_4}) \dots \delta(\mathbf{r}_{l_{2M-1}} - \mathbf{r}_{l_{2M}}), \end{aligned} \quad (1)$$

where $l_i = 1, 2, \dots, 2M$ and $l_i \neq l_j$ for all $i \neq j$, and \mathcal{N} is the Gaussian normalization.

If we introduce another field ϕ_2 , in terms of complex fields $\varphi = \phi_1 + i\phi_2$ and $\varphi^* = \phi_1 - i\phi_2$, the following identity

follows (see Fig. 1),

$$\begin{aligned}
J &= \mathcal{N}' \int [d\phi_1][d\phi_2] \prod_{i=1}^M [\phi_1(\mathbf{r}_i) + i\phi_2(\mathbf{r}_i)] \prod_{j=1}^{M'} [\phi_1(\mathbf{R}_j) - i\phi_2(\mathbf{R}_j)] e^{-\int d\mathbf{r} \phi_1^2(\mathbf{r}) - \int d\mathbf{r} \phi_2^2(\mathbf{r})} \\
&= \mathcal{N}' \int [d\varphi][d\varphi^*] \prod_{i=1}^M \varphi(\mathbf{r}_i) \prod_{j=1}^{M'} \varphi^*(\mathbf{R}_j) e^{-\int d\mathbf{r} \varphi(\mathbf{r}) \varphi^*(\mathbf{r})} \\
&= \delta_{M,M'} \sum_{\text{all pairing}} \delta(\mathbf{r}_{l_1} - \mathbf{R}_{m_1}) \delta(\mathbf{r}_{l_2} - \mathbf{R}_{m_2}) \dots \delta(\mathbf{r}_{l_M} - \mathbf{R}_{m_M}),
\end{aligned} \tag{2}$$

where l_i and m_i can vary over $(1, 2, \dots, M)$ with $l_i \neq l_j$ and $m_i \neq m_j$ for all $i \neq j$. This means that each φ is associated with another φ^* through a Dirac delta function in all possible pairwise combinations. As shown in Fig. 1, we can view the fields φ and φ^* as being complementary, since the delta-function connection does not occur between pairs of φ or pairs of φ^* . This Gaussian theory, therefore, enumerates all possible pairs of points \mathbf{r}_i and \mathbf{R}_j and enforces this by inserting a Dirac delta.

We consider a polymer chain consisting of N links (see Fig. 2). Given the Green function $G(\mathbf{r}, \mathbf{r}')$ for the segment of chain between two links, the conformation statistical weight of the polymer, whose conformation is described by the points $\{\mathbf{R}_i\}$, is

$$P(\{\mathbf{R}_i\}) = G(\mathbf{R}_1, \mathbf{R}_2)G(\mathbf{R}_2, \mathbf{R}_3)\dots G(\mathbf{R}_{N-1}, \mathbf{R}_N). \tag{3}$$

The polymer is immersed in an ideal mixture made up of two types of cross-linked particles (see Fig. 3) with functionalities a and b , respectively. We can also think of the chain segments as forming two types of clusters (closed-shell clusters, as for Janus particles [20]) called micelles and vesicles. What is important is the fixed functionality. The role of these clustering centers is to provide the links of a certain fixed functionality between polymer segments, thereby connecting a given number of segments of the polymer chain together. Then the partition function can be written as

$$Z_N = \sum_{N_1, N_a, N_b=0}^{\infty} \mathcal{Z}_{N_1, N_a, N_b}, \tag{4}$$

where $N = N_1 + aN_a + bN_b$ is the total number of polymer segments or of particles (since the field-theory requires that each segment must be paired with a particle) and

$$\begin{aligned}
\mathcal{Z}_{N_1, N_a, N_b} &= \mathcal{N} \int d\mathbf{R}_1 \dots d\mathbf{R}_N e^{-v \sum_{n,m=1}^N \delta(\mathbf{R}_n - \mathbf{R}_m)} \int [d\varphi][d\varphi^*] e^{-\int d\mathbf{r} \varphi(\mathbf{r}) \varphi^*(\mathbf{r})} \times \\
&\quad \varphi^*(\mathbf{R}_1) G(\mathbf{R}_1, \mathbf{R}_2) \varphi^*(\mathbf{R}_2) G(\mathbf{R}_2, \mathbf{R}_3) \dots G(\mathbf{R}_{N-1}, \mathbf{R}_N) \varphi^*(\mathbf{R}_N) \times \\
&\quad \frac{1}{N_1!} \left(\int d\mathbf{r} z_1 \varphi(\mathbf{r}) \right)^{N_1} \frac{1}{N_a!} \left(\int d\mathbf{r} z_a \varphi^a(\mathbf{r}) \right)^{N_a} \frac{1}{N_b!} \left(\int d\mathbf{r} z_b \varphi^b(\mathbf{r}) \right)^{N_b},
\end{aligned} \tag{5}$$

and the z_i are generalized fugacities (that might also contain a multiplicity associated with the functionality). We have explicitly added clusters of functionality one (the single particles) here to represent the “sea” of particles in which the polymer and the a and b clusters are immersed. Clearly clusters of size one simply link to a single polymer segment and therefore do not cause association as the a and b clusters do. Note that we are not interested in describing the precise model for the mechanism by which the clusters of a given functionality are formed from the aggregation of particles (more on this in Section VI); we just assume that this aggregation process takes place. At this level of description the physics of the precise mechanism for the multimerization resides in the fugacities. In our present formalism the clustering centers and the particles are pointlike. In principle it is also possible to extend the current formalism to model clusters of finite extension. We have also added an excluded volume term v , to the polymer chain, with the dimensions of a volume.

It is possible to use the formalism without necessarily introducing the essentially inert clusters of functionality one, which turns out to be the fugacity $z_1 = 1$ case of the equations derived below. Appendix D shows the details. We continue with the slightly more general formalism here, noting that $z_1 \rightarrow 1$ will show no effects due to the addition of these convenient clustering centers.

We then find in a short hand notation, and neglecting for the time being the excluded volume term,

$$Z_N = \mathcal{N} \int [d\varphi][d\varphi^*] \left\{ \prod d\mathbf{R} \right\} \left\{ \prod G \right\} \eta^N \exp \left(- \int d\mathbf{r} \varphi(\mathbf{r})\varphi^*(\mathbf{r}) + \int d\mathbf{r} \rho(\mathbf{r}) \ln(\varphi^*(\mathbf{r})/\eta) + z_1 \int d\mathbf{r} \varphi(\mathbf{r}) + z_a \int d\mathbf{r} \varphi^a(\mathbf{r}) + z_b \int d\mathbf{r} \varphi^b(\mathbf{r}) \right) \quad (6)$$

$$= \mathcal{N} \int [d\varphi][d\varphi^*] \left\{ \prod d\mathbf{R} \right\} \left\{ \prod G \right\} \exp\{\mathcal{F}[\varphi, \varphi^*]\}, \quad (7)$$

where we introduced the microscopic density of polymer links $\rho(\mathbf{r}) = \sum_{i=1}^N \delta(\mathbf{r} - \mathbf{R}_i)$ and η is an arbitrary constant with the dimensions of a length to the power $-3/2$. In the rest of the paper we will measure lengths in units of $\eta^{-2/3}$. A natural choice would be $\eta = \ell^{-3/2}$, with ℓ the Kuhn length of the polymer segment.

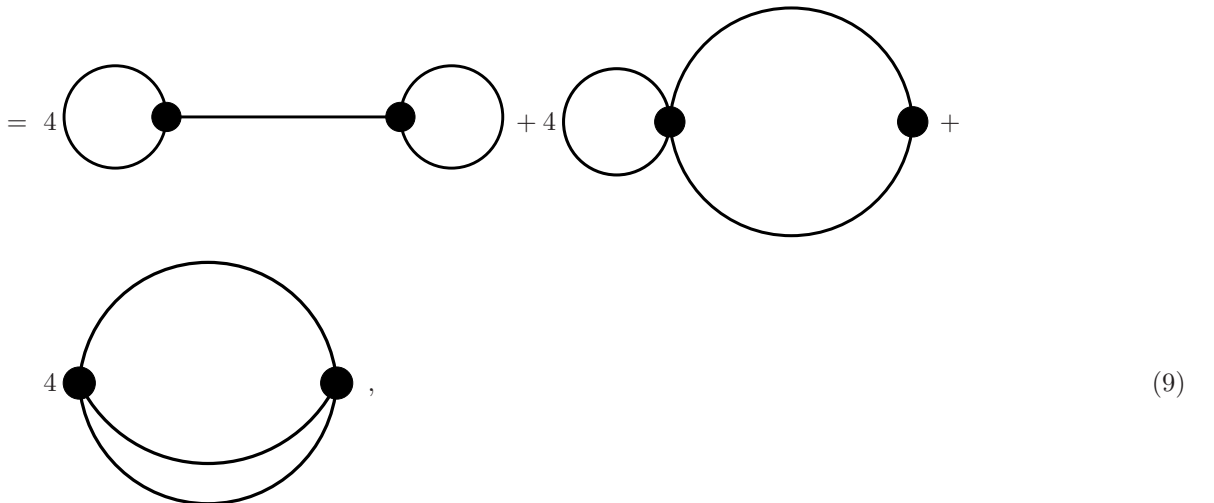
A. A simple example

To clarify our formalism we here consider the simple example of a polymer, with 4 polymer segments, interacting with two clustering centers of functionality $a = 2$. Using the properties of the Gaussian chains, the partition function, neglecting the excluded volume term, is written as

$$\begin{aligned} \mathcal{Z} &= \mathcal{N} \int [d\varphi][d\varphi^*] \left\{ \prod_{i=1}^4 d\mathbf{R}_i \right\} \left\{ \prod_{i=1}^2 d\mathbf{r}_i \right\} \left\{ \prod_{i=1}^3 G(\mathbf{R}_i, \mathbf{R}_{i+1}) \right\} e^{-\int d\mathbf{r} \varphi(\mathbf{r})\varphi^*(\mathbf{r})} \times \\ &\quad \left\{ \prod_{i=1}^4 \varphi^*(\mathbf{R}_i) \right\} z_2^2 \varphi^2(\mathbf{r}_1) \varphi^2(\mathbf{r}_2) \\ &= \mathcal{N} z_2^2 \int d\mathbf{r}_1 d\mathbf{r}_2 \sum' G(\mathbf{r}_{i_1}, \mathbf{r}_{i_2}) G(\mathbf{r}_{i_2}, \mathbf{r}_{i_3}) G(\mathbf{r}_{i_3}, \mathbf{r}_{i_4}) . \end{aligned} \quad (8)$$

where we used Eq. (2) and the prime on the last summation symbol indicates that we have to sum over all possible ways of assigning to the indexes (i_1, i_2, i_3, i_4) the set $(1, 1, 2, 2)$. We then see that the result is given by

$$\mathcal{Z} = \mathcal{N} z_2^2 \left[4 \int d\mathbf{r}_1 d\mathbf{r}_2 G(\mathbf{r}_1, \mathbf{r}_1) G(\mathbf{r}_1, \mathbf{r}_2) G(\mathbf{r}_2, \mathbf{r}_2) + 4 \int d\mathbf{r}_1 d\mathbf{r}_2 G(\mathbf{r}_1, \mathbf{r}_2) G(\mathbf{r}_2, \mathbf{r}_2) G(\mathbf{r}_2, \mathbf{r}_1) + 4 \int d\mathbf{r}_1 d\mathbf{r}_2 G(\mathbf{r}_1, \mathbf{r}_2) G(\mathbf{r}_2, \mathbf{r}_1) G(\mathbf{r}_1, \mathbf{r}_2) \right]$$



where lines represent polymer segments and black circles represent integration.

III. THE SADDLE POINT APPROXIMATION

We look at the saddle point equations for the fields φ and φ^* for any arbitrary yet fixed conformation of the polymer $\rho = \rho(\mathbf{r}) \geq 0 \forall \mathbf{r} \in \mathbb{R}^3$. The saddle point approximation becomes necessary because the field-theoretical formulation of the system, Eq. (6), is certainly highly non-Gaussian. We proceed to calculate the saddle point and note that, for fixed polymer conformation, the resulting condition is a set of algebraic equations, *i.e.* the saddle point depends only on the local density. We shall also see that there exists always exactly one saddle point, corresponding to the physical solution of the equations.

We need to determine the critical point $(\bar{\varphi}, \bar{\varphi}^*)$, which amounts to solving

$$\frac{\delta \mathcal{F}}{\delta \varphi(\mathbf{r})} \Big|_{\bar{\varphi}, \bar{\varphi}^*} = 0, \quad \frac{\delta \mathcal{F}}{\delta \varphi^*(\mathbf{r})} \Big|_{\bar{\varphi}, \bar{\varphi}^*} = 0 \quad (10)$$

or

$$-\bar{\varphi}^* + z_1 + az_a \bar{\varphi}^{a-1} + bz_b \bar{\varphi}^{b-1} = 0, \quad (11)$$

$$-\bar{\varphi} + \rho/\bar{\varphi}^* = 0. \quad (12)$$

These can be combined to give

$$-\rho/\bar{\varphi} + z_1 + az_a \bar{\varphi}^{a-1} + bz_b \bar{\varphi}^{b-1} = 0. \quad (13)$$

A. Properties of the solutions of the saddle point approximation

From Eq. (13) we can write

$$-\rho + f(\bar{\varphi}) = 0, \quad (14)$$

where $f(x) = z_1 x + az_a x^a + bz_b x^b$. We can then show that there exists at least one positive solution of Eq. (13) for $\rho > 0$. Indeed when $\bar{\varphi} \rightarrow 0$ then $-\rho + f(\bar{\varphi}) = -\rho < 0$, whereas when $\bar{\varphi} > \rho/z_1$ then $-\rho + f(\bar{\varphi}) > 0$. Consequently $-\rho + f(\bar{\varphi})$ goes through a zero when $\bar{\varphi} \in [0, \infty)$. And it is easy to show that there is exactly one positive solution $\bar{\varphi} > 0$ for any $\rho > 0$. $f'(\bar{\varphi}) = z_1 + a^2 z_a \bar{\varphi}^{a-1} + b^2 z_b \bar{\varphi}^{b-1}$ so $f'(\bar{\varphi}) > 0$ for all $\bar{\varphi} \geq 0$. Since the derivative is strictly positive and the polynomial goes from negative to positive, there exists exactly one positive root $\bar{\varphi}$ for any $\rho > 0$. As we show in Section IV B the local cluster densities of the saddle point are proportional to $z_1 \bar{\varphi}$, $az_a \bar{\varphi}^a$, and $bz_b \bar{\varphi}^b$, such that $\bar{\varphi}$ must be non-negative.

B. Solutions for $\bar{\varphi}$ and $\bar{\varphi}^*$

Consider the particular case $a = 2, b = 0$, corresponding to reversible crosslinking, then from Eq. (13) we find for the critical point

$$\bar{\varphi}_\pm = \frac{-z_1 \pm \sqrt{z_1^2 + 8z_2\rho}}{4z_2}, \quad (15)$$

$$\bar{\varphi}_\pm^* = \frac{4z_2\rho}{-z_1 \pm \sqrt{z_1^2 + 8z_2\rho}}, \quad (16)$$

which rules out the $\bar{\varphi}_-$ solution, as the logarithm of $\bar{\varphi}_-^*$ is not well defined.

C. Expansion of \mathcal{F} around the critical point

We can expand the function \mathcal{F} around the critical point to second order in the fluctuations $\Delta\varphi = \varphi - \bar{\varphi} = \Delta\phi_1 + i\Delta\phi_2$ and $\Delta\varphi^* = \varphi^* - \bar{\varphi}^* = \Delta\phi_1 - i\Delta\phi_2$,

$$\begin{aligned} \mathcal{F}[\bar{\varphi} + \Delta\varphi, \bar{\varphi}^* + \Delta\varphi^*] &= \mathcal{F}[\bar{\varphi}, \bar{\varphi}^*] + \\ &\quad \frac{1}{2} \int d\mathbf{r}_1 \int d\mathbf{r}_2 (\Delta\phi_1(\mathbf{r}_1) \Delta\phi_2(\mathbf{r}_1)) \cdot F_2(\mathbf{r}_1, \mathbf{r}_2) \cdot \begin{pmatrix} \Delta\phi_1(\mathbf{r}_2) \\ \Delta\phi_2(\mathbf{r}_2) \end{pmatrix} + \\ &\quad \text{third order terms,} \end{aligned} \quad (17)$$

where $F_2(\mathbf{r}_1, \mathbf{r}_2)$ is the following 2×2 matrix

$$F_2(\mathbf{r}_1, \mathbf{r}_2) = \begin{pmatrix} \frac{\delta^2 \mathcal{F}}{\delta \phi_1(\mathbf{r}_1) \delta \phi_1(\mathbf{r}_2)} & \frac{\delta^2 \mathcal{F}}{\delta \phi_1(\mathbf{r}_1) \delta \phi_2(\mathbf{r}_2)} \\ \frac{\delta^2 \mathcal{F}}{\delta \phi_2(\mathbf{r}_1) \delta \phi_1(\mathbf{r}_2)} & \frac{\delta^2 \mathcal{F}}{\delta \phi_2(\mathbf{r}_1) \delta \phi_2(\mathbf{r}_2)} \end{pmatrix}_{\bar{\varphi}, \bar{\varphi}^*}. \quad (18)$$

We have

$$\frac{\delta^2 \mathcal{F}}{\delta \phi_1(\mathbf{r}_1) \delta \phi_1(\mathbf{r}_2)} \Big|_{\bar{\varphi}, \bar{\varphi}^*} = \left[-2 - \frac{\rho}{\bar{\varphi}^{*2}} + a(a-1)z_a \bar{\varphi}^{a-2} + b(b-1)z_b \bar{\varphi}^{b-2} \right] \delta(\mathbf{r}_1 - \mathbf{r}_2), \quad (19)$$

$$\frac{\delta^2 \mathcal{F}}{\delta \phi_1(\mathbf{r}_1) \delta \phi_2(\mathbf{r}_2)} \Big|_{\bar{\varphi}, \bar{\varphi}^*} = i \left[\frac{\rho}{\bar{\varphi}^{*2}} + a(a-1)z_a \bar{\varphi}^{a-2} + b(b-1)z_b \bar{\varphi}^{b-2} \right] \delta(\mathbf{r}_1 - \mathbf{r}_2), \quad (20)$$

$$\frac{\delta^2 \mathcal{F}}{\delta \phi_2(\mathbf{r}_1) \delta \phi_2(\mathbf{r}_2)} \Big|_{\bar{\varphi}, \bar{\varphi}^*} = \left[-2 + \frac{\rho}{\bar{\varphi}^{*2}} - a(a-1)z_a \bar{\varphi}^{a-2} - b(b-1)z_b \bar{\varphi}^{b-2} \right] \delta(\mathbf{r}_1 - \mathbf{r}_2), \quad (21)$$

We can then introduce the matrix $\mathcal{M}[\rho]$ as

$$\begin{pmatrix} -2 - \frac{\rho}{\bar{\varphi}^{*2}} + a(a-1)z_a \bar{\varphi}^{a-2} + b(b-1)z_b \bar{\varphi}^{b-2} & i \left[\frac{\rho}{\bar{\varphi}^{*2}} + a(a-1)z_a \bar{\varphi}^{a-2} + b(b-1)z_b \bar{\varphi}^{b-2} \right] \\ i \left[\frac{\rho}{\bar{\varphi}^{*2}} + a(a-1)z_a \bar{\varphi}^{a-2} + b(b-1)z_b \bar{\varphi}^{b-2} \right] & -2 + \frac{\rho}{\bar{\varphi}^{*2}} - a(a-1)z_a \bar{\varphi}^{a-2} - b(b-1)z_b \bar{\varphi}^{b-2} \end{pmatrix}, \quad (22)$$

Then the partition function can be rewritten as

$$Z_N \approx \mathcal{N}' \int \left\{ \prod d\mathbf{R} \right\} \left\{ \prod G \right\} \exp\{M[\rho]\}, \quad (23)$$

where

$$M[\rho] = \mathcal{F}[\bar{\varphi}, \bar{\varphi}^*] - \frac{1}{2} \int d\mathbf{r} \ln \{\det \mathcal{M}[\rho]\}, \quad (24)$$

and

$$\det \mathcal{M}[\rho] = 4 [1 + z_a a(a-1) \bar{\varphi}^a / \rho + z_b b(b-1) \bar{\varphi}^b / \rho]. \quad (25)$$

For finite ρ the determinant is always positive with positive real parts of the eigenvalues, if $\bar{\varphi} > 0$. Hence the saddle point is stable.

As the density ρ increases we note that the free energy calculation due to the saddle point $\mathcal{F}[\bar{\varphi}, \bar{\varphi}^*]$ grows at least as ρ , but that the fluctuation contribution $-\frac{1}{2} \int d\mathbf{r} \ln \{\det \mathcal{M}[\rho]\}$ strives to a constant. Therefore at sufficiently high density we expect the relative contribution of the fluctuations to become negligible.

In the particular case $a = 2, b = 0$ we find

$$\det \mathcal{M}_{\pm}[\rho] = 4 (1 + 2z_2 \bar{\varphi}_{\pm} / \bar{\varphi}_{\pm}^*). \quad (26)$$

IV. THE RANDOM PHASE APPROXIMATION

In this section we express the polymer in terms of a segment density via the so-called random phase approximation. We restrict ourselves to the situations where the polymer segments are presumed to be distributed homogeneously with Gaussian density fluctuations around this value. For sufficiently dense systems this has been treated as a reasonable approximation [6] in permanently networked systems. We do not investigate the cases of possible inhomogeneous phases. In principle we would then need to expand our results in the preceding sections to higher orders in the density fluctuations [33–35] or attempt to express our results in terms of more complex quantities [46, 47]. However, we do investigate where our RPA with the homogeneity assumption fails as one indicator for possibly different phase behaviour in the system.

A. Basic formulation

Clearly our clustering formalism produces a significantly nontrivial density dependence. Presuming that our system behaves like a highly dense polymer melt, where the fluctuations of $\rho = \bar{\rho} + \Delta\rho$ are small, one can use the following Random Phase Approximation [35] (RPA) (see Appendix B),

$$\begin{aligned} \int \left\{ \prod d\mathbf{R} \right\} \left\{ \prod G \right\} \dots &= \mathcal{N}'' \int [d\Delta\rho] \exp \left(-\frac{1}{2} \int d\mathbf{r} \int d\mathbf{r}' \Delta\rho(\mathbf{r}) \frac{\tilde{S}_0^{-1}(|\mathbf{r} - \mathbf{r}'|)}{V} \Delta\rho(\mathbf{r}') \right) \dots \\ &= \mathcal{N}'' \int [d\Delta\tilde{\rho}] \exp \left(-\frac{1}{2} \frac{1}{V} \sum_{\mathbf{k}} \Delta\tilde{\rho}(\mathbf{k}) \frac{\tilde{S}_0^{-1}(k)}{V} \Delta\tilde{\rho}(-\mathbf{k}) \right) \dots , \end{aligned} \quad (27)$$

where we denoted with a tilde the Fourier transform [48] and with a hat an inverse Fourier transform. We note that this type of approach is not atypical in calculations for quenched gels [49].

Expanding to second order in the density fluctuations we find, from Eq. (24) and Eqs. (11)-(12),

$$\begin{aligned} M[\bar{\rho} + \Delta\rho] &= AV + B \int d\mathbf{r} \Delta\rho(\mathbf{r}) + C \int d\mathbf{r} [\Delta\rho(\mathbf{r})]^2 + \dots \\ &= AV + C \int d\mathbf{r} [\Delta\rho(\mathbf{r})]^2 + \dots , \end{aligned} \quad (28)$$

where we used the fact that $\int d\mathbf{r} \Delta\rho(\mathbf{r}) = 0$. V is the volume of the box, A, B , and C are given functions of z_1, z_2 , and $\bar{\rho}$ and for the particular case $a = 2, b = 0$ can be found in Appendix A. Notice that in this case A_- is not defined for any values of the average density so only the A_+, B_+ , and C_+ solution is physically meaningful, i.e. they correspond to the expected positive $\bar{\varphi}$ solution (see Section III A).

We then obtain the following approximation for the partition function of Eq. (23)

$$Z_N \approx \mathcal{N}''' e^{AV - \frac{1}{2} \int d\mathbf{r} \ln(\widehat{\tilde{S}_0^{-1}}/V - 2C)} , \quad (29)$$

where $\widehat{\tilde{S}_0^{-1}}$ is the operator whose \mathbf{r}, \mathbf{r}' component is given by $\widehat{\tilde{S}_0^{-1}}(|\mathbf{r} - \mathbf{r}'|)$.

In terms of the free energy density $\beta f = -\ln(Z_N)/V$ we find, in the thermodynamic limit ($V \rightarrow \infty$ with $\bar{\rho} = N/V$ constant),

$$\beta f = -A - \frac{1}{2} \ln(-2C) . \quad (30)$$

B. Local clustered segment densities

Following the usual method for grand-canonical ensemble it is possible to calculate the local densities of segments that form part of different sizes of clusters. We then compute

$$n_1 = \frac{z_1}{N} \frac{\partial \ln Z_N}{\partial z_1} , \quad (31)$$

for segments of the chain that are not cross-linked, and

$$n_x = x \frac{z_x}{N} \frac{\partial \ln Z_N}{\partial z_x} , \quad (32)$$

for the density of segments part of clusters of size x .

Neglecting the logarithmic corrections due to the quadratic fluctuations, we have

$$\ln Z_N = VA = M[\bar{\rho}] . \quad (33)$$

Within the saddle point approximation we split the contributions into parts due to the saddle point above and due to the quadratic fluctuations (notice that this analysis holds also locally at the level of the partition function for an

arbitrary $\rho = \rho(\mathbf{r})$ profile of polymer chain density)

$$\begin{aligned} n_x &= x \frac{z_x}{N} \frac{\partial \mathcal{F}[\bar{\varphi}, \bar{\varphi}^*] |_{\rho=\bar{\rho}}}{\partial z_x} - x \frac{z_x V}{2N} \frac{\partial \ln \det \mathcal{M}[\bar{\rho}]}{\partial z_x} \\ &= n_x^S + n_x^Q , \end{aligned} \quad (34)$$

where $x = 1, x = a$, or $x = b$. We then find

$$n_x^S = \frac{x z_x \bar{\varphi}^x}{\bar{\rho}} . \quad (35)$$

Since n_x^S have to be real and non-negative, in the saddle point approximation, also the solutions $\bar{\varphi}$ have to be real and non-negative. Immediately from the saddle point equation (13) follows that

$$n_1^S + n_a^S + n_b^S = 1 , \quad (36)$$

must hold generally. We also find after some algebra

$$n_1^Q + n_a^Q + n_b^Q = 0 . \quad (37)$$

This means that the saddle point approximation conserves the total number of segments for any density. Consequently, any average over these density dependent expressions, irrespective of the approximation, must satisfy the conservation. However we note that the conservation laws (36) and (37) do not prevent possibly negative $n_x^S + n_x^Q$ which can arise in the region where the fluctuation part is not sufficiently smaller than the saddle point. As the validity of the saddle point improves with density, also this possibility disappears.

For the special case $a = 2, b = 0$ we have

$$n_1^S = \frac{2z_1}{z_1 + \sqrt{z_1^2 + 8z_2\bar{\rho}}} , \quad (38)$$

$$n_1^Q = \frac{z_1(-z_1 + \sqrt{z_1^2 + 8z_2\bar{\rho}})}{2\bar{\rho}(z_1^2 + 8z_2\bar{\rho})} , \quad (39)$$

as a consequence we see that the fraction of monomers not in a cross-link decreases with the density.

C. The effective potential

Upon integrating over the degrees of freedom associated with the clustering centers the remaining integral in the partition function is that over the polymer density degrees of freedom (in the RPA). This permits us to interpret the effective interaction between polymer segments as caused by the clustering. It consists of the typically attractive contribution to the polymer-polymer quadratic density fluctuations from the aggregating fields and any direct polymer-polymer interaction (such as excluded volume interactions).

From Eq. (23) and (27)-(28) we can rewrite the partition function as

$$Z_N \approx \mathcal{N}''' \int [d\Delta\rho] e^{-\frac{1}{2} \int d\mathbf{r} \int d\mathbf{r}' \Delta\rho(\mathbf{r}) \frac{\tilde{S}_0^{-1}(\mathbf{r}-\mathbf{r}')}{V} \Delta\rho(\mathbf{r}')] e^{AV} e^{-\frac{1}{2} \int d\mathbf{r} \int d\mathbf{r}' \Delta\rho(\mathbf{r}) W(\mathbf{r}-\mathbf{r}') \Delta\rho(\mathbf{r}')} \quad (40)$$

where the effective potential between the polymer segments, W , is given by

$$W(\mathbf{r} - \mathbf{r}') = - \left. \frac{\delta^2 M[\rho]}{\delta \rho(\mathbf{r}) \delta \rho(\mathbf{r}')} \right|_{\rho(\mathbf{r})=\bar{\rho}} = -2C(z_1, z_a, z_b; \bar{\rho}) \delta(\mathbf{r} - \mathbf{r}') . \quad (41)$$

We can then split the contribution from the saddle point and the quadratic contribution of Eq. (24) and write

$$C = C_S + C_Q , \quad (42)$$

$$C_S = \frac{1}{2} \left. \frac{\partial^2 f^S(\bar{\varphi}, \rho)}{\partial \rho^2} \right|_{\rho=\bar{\rho}} , \quad (43)$$

$$C_Q = \frac{1}{2} \left. \frac{\partial^2 f^Q(\bar{\varphi}, \rho)}{\partial \rho^2} \right|_{\rho=\bar{\rho}} , \quad (44)$$

where

$$f^S = -\rho + \rho \ln(\rho/\bar{\varphi}) + z_1 \bar{\varphi} + z_a \bar{\varphi}^a + z_b \bar{\varphi}^b , \quad (45)$$

$$f^Q = -\frac{1}{2} \ln[4(1+a(a-1)z_a \bar{\varphi}^a/\rho + b(b-1)\bar{\varphi}^b/\rho)] . \quad (46)$$

Now, using Eq. (13), we find $\partial f^S/\partial\rho = \ln\rho - \ln\bar{\varphi}$ and, using the property $\partial\bar{\varphi}/\partial\rho = 1/(z_1 + a^2 z_a \bar{\varphi}^{a-1} + b^2 z_b \bar{\varphi}^{b-1})$, follows $\partial^2 f^S/\partial\rho^2 = 1/\rho - 1/(z_1 \bar{\varphi} + z_a a^2 \bar{\varphi}^a + z_b b^2 \bar{\varphi}^b)$. Let us assume for definiteness that $b > a$. Then when ρ is very small $z_1 \bar{\varphi} \approx \rho$ and $\partial^2 f^S/\partial\rho^2 \approx a(a-1)(z_a/z_1^a) \rho^{a-2}/[1 - a(z_a/z_1^a) \rho^{a-1}]$, while when ρ is very large $z_b b \bar{\varphi}^b \approx \rho$ so that $\partial^2 f^S/\partial\rho^2 \approx (b-1)/(b\rho)$. Moreover we find in the large ρ limit that $\partial^2 f^Q/\partial\rho^2$ behaves at least as $1/\rho^2$.

We remark that in the small ρ limit in the $a = 2, b = 0$ case $\partial^2 f^Q/\partial\rho^2 \approx 10z_a^2/z_1^4$ whereas in the $a = 10, b = 40$ case $\partial^2 f^Q/\partial\rho^2 \approx -3240z_a \rho^7/z_1^{10}$. However we guard against interpreting this as a repulsive interaction as the saddle point approximation to our field-theory is not expected to be accurate at small densities. This repulsive contribution in the small density limit for the effective potential of the Janus case (see Section VI) explains the fact that here the RPA can be valid (see Section IV D) even if we do not add any excluded volume interaction to the polymer.

For the simple case $a = 2, b = 0$ we then find that $C_+ = C_S + C_Q$ where

$$C_S = \frac{1}{4\bar{\rho}} \left(1 - \frac{z_1}{\sqrt{z_1^2 + 8z_2\bar{\rho}}} \right) , \quad (47)$$

$$C_Q = \frac{1}{8\bar{\rho}^2} \left[\frac{64(\bar{\rho}z_2)^2}{(z_1^2 + 8z_2\bar{\rho})^2} - 1 + \frac{z_1^3 + 12z_1 z_2 \bar{\rho}}{(z_1^2 + 8z_2\bar{\rho})^{3/2}} \right] . \quad (48)$$

Here we also find in the small $\bar{\rho}$ limit

$$C_S = \frac{z_2}{z_1^2} - \frac{6z_2^2}{z_1^4} \bar{\rho} + O(\bar{\rho}^2) , \quad (49)$$

$$C_Q = \frac{5z_2^2}{z_1^4} - \frac{88z_2^3}{z_1^6} \bar{\rho} + O(\bar{\rho}^2) , \quad (50)$$

which tells us that the energy to cross-link goes to a constant proportional to z_2 .

In the large $\bar{\rho}$ limit

$$C_S = \frac{1}{4\bar{\rho}} - \frac{z_1}{8\sqrt{2z_2}\bar{\rho}^{3/2}} + \frac{z_1^3}{128\sqrt{2z_2^3}\bar{\rho}^{5/2}} + O(\bar{\rho}^{-3}) , \quad (51)$$

$$C_Q = \frac{3z_1}{32\sqrt{2z_2}\bar{\rho}^{5/2}} + O(\bar{\rho}^{-3}) , \quad (52)$$

which tells us that the energy to cross-link goes to zero as $1/\bar{\rho}$, in accord with the fact that we are in a dense system.

The effective potential calculated here, based on small density fluctuations around a background of a given density, is dependent on the average density. As expected the clustering produces a local attractive interaction.

However, it is interesting to note that the strength of this interaction decreases with average density. We attribute this to the fact that the fraction of free segments (i.e. those in clusters of size 1) decreases with the average density according to Eq. (38). Therefore, for large $\bar{\rho}$, the number of additional free segments gained by increasing the density from $\bar{\rho}$ to $\bar{\rho} + \Delta$ is proportional to $\bar{\rho}^{-1/2}$ leading to a pairwise contribution $\Delta^2/\bar{\rho}$ as found in Eq. (51).

D. Validity of RPA

The RPA is based on a homogeneity assumption which no longer holds when the RPA itself predicts overly large fluctuations. In order to obtain Eq. (29) we must have that $\tilde{S}_0^{-1}(k)/V - 2C$ is a strictly positive function for all values of the wave vector k . Since $\tilde{S}_0^{-1}(k)$ is a monotonically increasing function of k , the RPA will be valid as long as

$$C < \frac{\tilde{S}_0^{-1}(0)}{2V} = \frac{1}{2V\bar{\rho}^2} . \quad (53)$$

In the thermodynamic limit one would require that $C < 0$, for the validity of RPA.

We can then extend the region of the validity of RPA by adding an excluded volume effect [50] to the polymer which amounts to taking $M[\rho] \rightarrow M[\rho] - v \int d\mathbf{r} \rho^2(\mathbf{r})$ with v a positive constant with the dimensions of a volume. We will then have

$$A \rightarrow A - \bar{\rho}^2 v, \quad B \rightarrow B - 2\bar{\rho}v, \quad C \rightarrow C - v, \quad (54)$$

and the validity of RPA becomes $C < v$.

For the $a = 2, b = 0$ case we have that C_+ is always positive so the RPA cannot be applied without the excluded volume interaction. As a matter of fact we have $\lim_{\bar{\rho} \rightarrow \infty} C_+ = 0$ and $\lim_{\bar{\rho} \rightarrow 0} C_+ = z_2(z_1^2 + 5z_2)/z_1^4$ and C_+ is a monotonically decreasing function of $\bar{\rho}$. So by choosing v any arbitrarily small positive constant we are able to extend the range of validity of RPA to arbitrarily large densities.

In this case choosing $z_1 = 1, z_2 = e^{2\beta}$, and $v = 1$ the validity domain in the phase diagram is determined in Fig. 4.

In Fig. 5 we show the behavior of the free energy density as a function of density in the case $a = 2, b = 0$. Here we choose $z_1 = 1, z_2 = e^{2\beta}$ were $\beta = 1/k_B T$ with k_B Boltzmann constant and T is the temperature and $v = 1$.

V. THE STATIC STRUCTURE FACTOR

The Fourier transform of the pair correlation function is defined as [51]

$$\tilde{g}(\mathbf{k}) = \frac{1}{N} \langle \tilde{\rho}(\mathbf{k}) \tilde{\rho}(-\mathbf{k}) \rangle = \frac{1}{N} \langle \Delta \tilde{\rho}(\mathbf{k}) \Delta \tilde{\rho}(-\mathbf{k}) \rangle, \quad \mathbf{k} \neq 0. \quad (55)$$

The quantity $\tilde{g}(\mathbf{k})$ can be measured experimentally by light scattering. Moreover one can extract some important information on the polymer properties from the small $k = |\mathbf{k}|$ behavior:

$$\tilde{g}(\mathbf{k}) = \tilde{g}(0) \left(1 - \frac{k^2}{3} R_g^2 + \dots \right), \quad (56)$$

where R_g is the radius of gyration of the polymer, namely

$$R_g^2 = \frac{1}{2N^2} \sum_{n=1}^N \sum_{m=1}^N \langle (\mathbf{R}_n - \mathbf{R}_m)^2 \rangle. \quad (57)$$

Now using the result from the RPA we find

$$N\tilde{g}(k) = V[\tilde{S}_0^{-1}(k)/V - 2C]^{-1}, \quad (58)$$

which when $C = -v$, agrees with Edwards' result [50, 52] for polymer chains with only excluded volume interactions [53]. Notice that the effective potential C is in general a function of $\bar{\rho}, z_1, z_a$, and z_b . As shown in Section IV C, $C + v$ tends to be positive (attractive interaction between polymer segments) in the presence of clustering centers. So we expect there to be a regime of density for which there is a balance between the repulsion due to the excluded volume effect and the attraction due to clustering making $C \approx 0$. In such case our result reproduces the one for the ideal chain (see section 1.2.3 in Ref. [51]).

In the small k limit we find

$$N\tilde{g}(k) = \frac{V^2}{1/\bar{\rho}^2 - 2CV} \left[1 - \frac{k^2}{3} \xi^2 + \dots \right], \quad (59)$$

where $\bar{\rho} = N/V$ is the average polymer segment density for a single long polymer chain and the “curvature” of the structure factor at $k = 0$ is

$$\xi^2 = \frac{\ell^2 \bar{\rho} V}{6 - 12\bar{\rho}^2 CV}, \quad (60)$$

where ℓ is the Kuhn length of the polymer. And in the thermodynamic limit

$$(\xi/\ell)^2 \rightarrow -\frac{1}{12\bar{\rho}C}. \quad (61)$$

So that at large polymer densities the curvature tends to a constant (we note that C now includes the excluded volume as in Eq. (54)).

We also find, in the thermodynamic limit, the following expression for the structure factor

$$g(k) \rightarrow \frac{12}{(\ell k)^2 - 24\bar{\rho}C} . \quad (62)$$

Notice that in the absence of the effective interaction ($C = 0$) the structure factor diverges at $k = 0$.

In the $a = 2, b = 0$ case, at constant V , in the small N limit we find the free polymer result $\xi^2 = N\ell^2/6 + O(N^3)$. In the large N limit we find

$$(\xi/\ell)^2 = \frac{1}{12v} \frac{V}{N} + \frac{1}{48v^2} \frac{V^2}{N^2} + O(1/N^{5/2}) . \quad (63)$$

Given the densest possible filling $N/V \sim 1/v$ the curvature tends to a constant.

VI. THE JANUS CASE

Although our field-theoretical formulation includes no precise model for the mechanism that causes clustering centers of a given functionality to occur, we investigate here the case where the functionalities (10 and 40) of the clustering centers are the same as those determined for Janus particles in recent studies. Indeed there has recently been much development in the techniques for the synthesis of new patchy colloidal particles [36–39]. One particularly simple class of these anisotropic particles, called Janus particles [40–43], seem to form mainly clusters of either 10 or 40 particles. Here Monte Carlo simulations [20, 21] indicate that mainly stable micelle (10 particles) or vesicle (40 particles) arrangements of these particles are to be found in the vapor phase. Moreover it was found that the clusters behave very similarly to an ideal gas, since the particles forming the cluster tend to arrange with their active surfaces towards the cluster center.

Janus chains have been suggested as potentially useful candidates for understanding interesting polymer phenomena [44]. We will apply our formalism to the case of a dense polymer in a Janus fluid and in so doing we hope to add to the recent interest for Janus particles interacting with polymer chains [43–45]. To the best of our knowledge there is no results in the literature that proves the clustering in the Janus fluid in the presence of the polymer. So we will take as a working hypothesis the existence of such a clustering. And make the approximation of treating the backbone units of the polymer (the Janus particles) as an ideal fluid.

Given the general setting described above we can apply our theoretical model to a polymer in a Janus fluid. By this we think of chain segments only clustering to form limited closed shell conformations, *i.e.* micelles and vesicles. As mentioned before, we however do not consider the nature of spacial extent of the clustering in detail and simply presume that it still occurs in the same way as if the Janus particles were not connected to the polymer.

In the Janus case we have to choose $a = 10$ and $b = 40$ (see Fig. 3). We then find for the determination of the critical point an algebraic equation of degree 40, Eq. (13). As expected, this equation has just one solution for which A (from Eq. (28)) is real and non-negative.

We can see the generalized fugacities defined as $z_i \propto \exp(-\beta u_i + \beta \mu_i)$ for $i = 1, 10, 40$, where u_i is the average internal energies of the cluster of i Janus particles and μ_i is the chemical potential of this cluster species. It is moreover reasonable to take $\mu_i \approx \mu$ independent of i (μ being the chemical potential of the vapor phase of the Janus fluid) so that we get $z_i \propto \exp(-\beta u_i)$.

Choosing $z_1 = 1, z_{10} = e^{10\beta}$, and $z_{40} = e^{40\beta}$ we find that at small densities (where the theory is expected to be not good) the effective potential is repulsive (due to the quadratic fluctuations in the theory) even without adding an excluded volume to the polymer (see Section IV C). The range of validity of RPA in the phase diagram is shown in Fig. 6. In the same Figure we show the behavior of the free energy density which clearly shows the signature for the breakdown of the RPA theory at high density.

Notice that, also in this case, $\lim_{\bar{\rho} \rightarrow \infty} C = 0$ so that by adding a small excluded volume will allow to reach the high densities domain with RPA. At a fixed temperature C , as a function of density, has a global maximum, so that choosing the excluded volume v bigger than this value, the RPA can be made valid at any density (see Fig. 7). Moreover we expect the theory to give consistent results in the high density regime.

Our choice for the fugacities is justified a posteriori since for $\beta < 1$ we are in the high temperature regime of the Janus vapor [20] where the internal energy of a cluster of i Janus particles is with a good approximation given by $-(i-1) \approx -i$ (corresponding to a completely stretched cluster).

Since Z_N is a grand-canonical in the clusters of Janus particles, we can take derivatives with respect to the generalized fugacity z_i to determine the concentration n_i of clusters of i Janus particles as follows

$$n_i = \frac{i\langle N_i \rangle}{N} = \frac{i}{N} \frac{\partial \ln Z_N}{\partial \ln z_i} , \quad (64)$$

where $\ln Z_N = V[A + \ln(-2C)/2]$.

A graph of the concentrations as a function of the average polymer density is shown in Fig. 8. From Fig. 8 one can see the difference between $n_x = n_x^S$ and $n_x = n_x^S + n_x^Q$ for $x = 1, 10$, and 40 and $\beta = 1$. Note that the conservation of particles $n_1 + n_{10} + n_{40} = 1$ is exactly satisfied at all densities and temperatures in both cases. In Fig. 9 we show the dependence of the concentrations from the temperature. We thus would say that at sufficiently high densities the vesicles appear and as a consequence the micelles are reduced.

We conclude that this suggests strong dominance of non-clustering at low densities. As the density is increased smaller clusters and eventually larger clusters dominate the linking behavior.

VII. CONCLUSIONS

In this work we have studied and developed a field-theoretical formalism for a polymer immersed in an ideal mixture of clustering centers. These centers cause clustering of either a particles or b particles, *i.e.* clusters of either species are monodisperse. The field-theory couples fields associated with stickers to the polymer chain density and provides a formally exact expression for the partition function (canonical in polymer and grand-canonical for the clustering centers). We showed that it is possible to compute quantities using the nonlinear theory by means of a saddle point approximation and we argue that the approximation improves as the density of the polymer chain increases. The current system and the choice of implementation of additional fields enabled us to derive saddle-point equations that are simpler than those that arise in some other formalisms by not requiring the solution of nonlinear integral equations. The benefit of the local saddle-point equations is that they also enable a relatively simple analysis of the stability and applicability considerations of the theory.

For a homogeneous, dense polymer system, we computed the effective interaction potential (up to quadratic density fluctuations) and computed properties of the structure factor within the random phase approximation. As expected, the addition of an excluded volume interaction will compensate for the attraction due to aggregation effects and extend the validity of the RPA. The effective pairwise potential obtained in this approximation has interesting, nontrivial density dependence. Another clear consequence of increasing chain density is the growing dominance of the higher-functional clustering centers.

The nature of the clustering process is definitely of importance in aggregating polymer systems. (Recently, a theory for cluster formation in homopolymer melts was introduced by Semenov [17].) One motivation for our study is the closed multimerization scenario suggested by particles in a Janus fluid, where micelles ($a = 10$) and vesicles ($b = 40$) are known to occur [20, 21]. Future work will focus the attention on the stability of such Janus-type multimers when connected to a polymer with more detailed models of the cluster itself.

Appendix A: Coefficients A, B , and C for the $a = 2, b = 0$ case

The A, B , and C coefficients are given by

$$A_{\pm} = \frac{1}{8z_2} \left\{ -z_1^2 \pm z_1 \sqrt{z_1^2 + 8\bar{\rho}z_2} + 8\bar{\rho}z_2 \ln \left(\frac{4\bar{\rho}z_2}{-z_1 \pm \sqrt{z_1^2 + 8\bar{\rho}z_2}} \right) + 4z_2 \left[\bar{\rho} + \ln \left(1 \pm \frac{z_1}{\sqrt{z_1^2 + 8\bar{\rho}z_2}} \right) - \ln 8 \right] \right\}, \quad (\text{A1})$$

$$B_{\pm} = -\frac{2z_2}{z_1^2 + 8\bar{\rho}z_2} + \frac{1}{4\bar{\rho}} \left(1 \mp \frac{z_1}{\sqrt{z_1^2 + 8\bar{\rho}z_2}} \right) + \ln \left(\frac{4\bar{\rho}z_2}{-z_1 \pm \sqrt{z_1^2 + 8\bar{\rho}z_2}} \right), \quad (\text{A2})$$

$$C_{\pm} = \frac{8z_2^2}{(z_1^2 + 8\bar{\rho}z_2)^2} + \frac{1}{8\bar{\rho}^2} \left[-1 \pm \frac{z_1}{\sqrt{z_1^2 + 8\bar{\rho}z_2}} + \bar{\rho} \left(2 \mp \frac{2z_1(z_1^2 - 2z_2 + 8\bar{\rho}z_2)}{(z_1^2 + 8\bar{\rho}z_2)^{3/2}} \right) \right]. \quad (\text{A3})$$

Appendix B: The Random Phase Approximation

For the polymer chain, with a Kuhn length ℓ , we can write

$$\begin{aligned} & \int \left\{ \prod d\mathbf{R} \right\} \left\{ \prod G \right\} = \\ & \int [d\rho] \int [d\zeta] \int [d\mathbf{R}] e^{-\frac{3}{2\ell} \int_0^L ds \dot{\mathbf{R}}^2(s)} e^{i \int dr \zeta(\mathbf{r}) [\rho(\mathbf{r}) - \int_0^L \frac{ds}{\ell} \delta(\mathbf{r} - \mathbf{R}(s))]} = \\ & \int [d\rho] \int [d\zeta] \int [d\mathbf{R}] e^{-\frac{3}{2\ell} \int_0^L ds \dot{\mathbf{R}}^2(s)} e^{i \int dr \zeta(\mathbf{r}) \rho(\mathbf{r})} \left[1 - i \int dr \int_0^L \frac{ds}{\ell} \zeta(\mathbf{r}) \delta(\mathbf{r} - \mathbf{R}(s)) - \right. \\ & \left. \frac{1}{2} \int dr \int_0^L \frac{ds}{\ell} \zeta(\mathbf{r}) \delta(\mathbf{r} - \mathbf{R}(s)) \int dr' \int_0^L \frac{ds'}{\ell} \zeta(\mathbf{r}') \delta(\mathbf{r}' - \mathbf{R}(s')) + \dots \right], \end{aligned} \quad (\text{B1})$$

where $L = N\ell$ is the total polymer length and the dot denotes a derivative with respect to s .

Now the first term gives just a normalization constant \mathcal{N} . To calculate the second term we introduce the polymer center of mass \mathbf{R}_0 so that $\mathbf{R}(s) = \mathbf{R}_0 + \Delta\mathbf{R}(s)$ and write

$$\begin{aligned} & \int [d\zeta] \int [d\mathbf{R}] e^{-\frac{3}{2\ell} \int_0^L ds \dot{\mathbf{R}}^2(s)} e^{i \int dr \zeta(\mathbf{r}) \rho(\mathbf{r})} \int dr \int_0^L \frac{ds}{\ell} \zeta(\mathbf{r}) \delta(\mathbf{r} - \mathbf{R}(s)) = \\ & \int [d\zeta] \int [d\mathbf{R}] e^{-\frac{3}{2\ell} \int_0^L ds \dot{\mathbf{R}}^2(s)} e^{i \int dr \zeta(\mathbf{r}) \rho(\mathbf{r})} \int dr \int_0^L \frac{ds}{\ell} \zeta(\mathbf{r}) \frac{1}{V} \sum_{\mathbf{k}} e^{i\mathbf{k}\mathbf{r} - i\mathbf{k}\mathbf{R}(s)} = \\ & \int [d\zeta] \int [d\Delta\mathbf{R}] \int d\mathbf{R}_0 e^{-\frac{3}{2\ell} \int_0^L ds \Delta\dot{\mathbf{R}}^2(s)} e^{i \int dr \zeta(\mathbf{r}) \rho(\mathbf{r})} \int dr \int_0^L \frac{ds}{\ell} \frac{1}{V} \sum_{\mathbf{k}} \zeta(\mathbf{r}) e^{i\mathbf{k}\mathbf{r}} e^{-i\mathbf{k}(\mathbf{R}_0 + \Delta\mathbf{R}(s))} = \\ & \int [d\zeta] e^{i \int dr \zeta(\mathbf{r}) \rho(\mathbf{r})} \mathcal{N} \frac{1}{V} \int dr \int_0^L \frac{ds}{\ell} \sum_{\mathbf{k},0} \zeta(\mathbf{r}) \delta_{\mathbf{k},0} = \\ & \int [d\zeta] e^{i \int dr \zeta(\mathbf{r}) \rho(\mathbf{r})} \mathcal{N} \frac{N}{V} \int dr \zeta(\mathbf{r}), \end{aligned} \quad (\text{B2})$$

where V is the volume of the box and $\delta_{\mathbf{k},0}$ is the Kronecker delta.

The third term gives

$$\begin{aligned} & \int [d\zeta] e^{i \int dr \zeta(\mathbf{r}) \rho(\mathbf{r})} \int [d\Delta\mathbf{R}] \int d\mathbf{R}_0 e^{-\frac{3}{2\ell} \int_0^L ds \Delta\dot{\mathbf{R}}^2(s)} \frac{1}{V^2} \sum_{\mathbf{k}} \sum_{\mathbf{k}'} \int dr \int_0^L \frac{ds}{\ell} \int dr' \int_0^L \frac{ds'}{\ell} \times \\ & \zeta(\mathbf{r}) \zeta(\mathbf{r}') e^{i\mathbf{k}\mathbf{r}} e^{i\mathbf{k}'\mathbf{r}'} e^{i(\mathbf{k}+\mathbf{k}')\mathbf{R}_0} e^{i\mathbf{k}\Delta\mathbf{R}(s)} e^{i\mathbf{k}'\Delta\mathbf{R}(s')} = \\ & \int [d\zeta] e^{i \int dr \zeta(\mathbf{r}) \rho(\mathbf{r})} \mathcal{N} \frac{1}{V^2} \int_0^L \frac{ds}{\ell} \int_0^L \frac{ds'}{\ell} \sum_{\mathbf{k}} \tilde{\zeta}(\mathbf{k}) \tilde{\zeta}(-\mathbf{k}) \left\langle e^{i\mathbf{k}(\mathbf{R}(s) - \mathbf{R}(s'))} \right\rangle_0, \end{aligned} \quad (\text{B3})$$

where we denoted with the average

$$\langle \dots \rangle_0 = \frac{\int [d\mathbf{R}] e^{-\frac{3}{2\ell} \int_0^L ds \dot{\mathbf{R}}^2(s)} [\dots]}{\int [d\mathbf{R}] e^{-\frac{3}{2\ell} \int_0^L ds \dot{\mathbf{R}}^2(s)}}, \quad (\text{B4})$$

and with the tilde the Fourier transform [48].

Now the average $\left\langle e^{i\mathbf{k}(\mathbf{R}(s) - \mathbf{R}(s'))} \right\rangle_0$ can be easily calculated by discretizing the polymer and integrating over the bond vectors $\mathbf{b}_i = \mathbf{R}_{i+1} - \mathbf{R}_i$, as follows

$$\left\langle e^{i\mathbf{k}(\mathbf{R}(s) - \mathbf{R}(s'))} \right\rangle_0 = \frac{\int \prod_i d\mathbf{b}_i e^{-\frac{3}{2\ell^2} \sum_i \mathbf{b}_i^2} e^{i\mathbf{k}(\mathbf{b}_1 + \mathbf{b}_2 + \dots + \mathbf{b}_n)}}{\int \prod_i d\mathbf{b}_i e^{-\frac{3}{2\ell^2} \sum_i \mathbf{b}_i^2}} = \left(e^{-\frac{\ell^2 \ell^2}{6}} \right)^n, \quad (\text{B5})$$

where $n = |s - s'|/\ell$. Since

$$\int_0^L ds \int_0^L ds' e^{-a|s-s'|} = \frac{2(aL - 1 + e^{-aL})}{a^2}, \quad (\text{B6})$$

we can introduce the function

$$\tilde{S}_0(k) = \frac{72(k^2\ell L/6 - 1 + e^{-\frac{k^2\ell L}{6}})}{V^2 k^4 \ell^4}, \quad (\text{B7})$$

with $\tilde{S}_0(0) = (N/V)^2 = \bar{\rho}^2$.

Then the expression we started with in Eq. (B1) can be rewritten, omitting the functional integral over the density collective variable, as

$$\mathcal{N} \int [d\tilde{\zeta}] e^{\frac{i}{V} \sum_{\mathbf{k}} \tilde{\zeta}(\mathbf{k}) \tilde{\rho}(-\mathbf{k})} \left[1 - i \frac{N}{V} \tilde{\zeta}(0) - \frac{1}{2V} \sum_{\mathbf{k}} \tilde{\zeta}(\mathbf{k}) V \tilde{S}_0(k) \tilde{\zeta}(-\mathbf{k}) + \dots \right]. \quad (\text{B8})$$

We can now reconstruct the exponential to obtain,

$$\begin{aligned} \int [d\tilde{\zeta}] e^{\frac{i}{V} \sum_{\mathbf{k}} \tilde{\zeta}(\mathbf{k}) \tilde{\rho}(-\mathbf{k})} e^{-\frac{1}{2V} \sum_{\mathbf{k}} \tilde{\zeta}(\mathbf{k}) V \tilde{S}_0(k) \tilde{\zeta}(-\mathbf{k}) - i \frac{N}{V} \tilde{\zeta}(0)} = \\ \mathcal{N}' e^{-\frac{1}{2V} \sum_{\mathbf{k}} \ln(\tilde{S}_0(k)V) e^{-\frac{1}{2V} \sum_{\mathbf{k}} \Delta \tilde{\rho}(\mathbf{k}) \frac{\tilde{S}_0^{-1}(k)}{V} \Delta \tilde{\rho}(-\mathbf{k})}}. \end{aligned} \quad (\text{B9})$$

Here $\Delta \tilde{\rho}(\mathbf{k}) = \tilde{\rho}(\mathbf{k}) - \bar{\rho}V\delta_{\mathbf{k},0}$.

Appendix C: The Gaussian distribution

The Gaussian distribution function for a set of real variables x_1, x_2, \dots, x_N is defined as

$$\Psi(x_1, x_2, \dots, x_N) = C \exp \left[-\frac{1}{2} \sum_{n,m} A_{nm} x_n x_m \right], \quad (\text{C1})$$

where A_{nm} is a symmetric positive definite matrix and C is a normalization constant given by the requirement $\int_{-\infty}^{\infty} \dots \int_{-\infty}^{\infty} \prod_n dx_n \Psi = 1$.

Let $\langle \dots \rangle$ be the average of the distribution function of Eq. (C1),

$$\langle \dots \rangle = \int_{-\infty}^{\infty} \dots \int_{-\infty}^{\infty} \prod_n dx_n \dots \Psi(x_1, x_2, \dots, x_N), \quad (\text{C2})$$

then, it can be proved [50], that

$$\langle x_n x_m \rangle = [A^{-1}]_{nm}. \quad (\text{C3})$$

In general we have the following formula (Wick's theorem)

$$\langle x_{n_1} x_{n_2} \dots x_{n_{2p}} \rangle = \sum_{\text{all pairing}} \langle x_{m_1} x_{m_2} \rangle \langle x_{m_3} x_{m_4} \rangle \dots \langle x_{m_{2p-1}} x_{m_{2p}} \rangle. \quad (\text{C4})$$

If the subscript n of x_n is regarded as a continuous variable, the set of points (x_1, x_2, \dots, x_N) represents a continuous function, and the integral over the set (x_1, x_2, \dots, x_N) reduces to the integration over all the function, and it is called the *functional integral*. It is denoted by the symbol $[dx]$, i.e. $\int \prod_n dx_n \dots \rightarrow \int [dx] \dots$

Consider now the following Gaussian distribution functional

$$\Psi[\phi] = C \exp \left[-\frac{1}{2} \int_{-\infty}^{\infty} dx \phi^2(x) \right], \quad (\text{C5})$$

where ϕ is a real function, then using the continuous limit of Eq. (C3) we find

$$\langle \phi(x) \phi(x') \rangle = \delta(x - x'). \quad (\text{C6})$$

where δ is the Dirac delta function.

If now $\phi = \phi_1 + i\phi_2$ is a complex function we consider the Gaussian distribution functional

$$\Psi[\phi, \phi^*] = C \exp \left[- \int_{-\infty}^{\infty} dx \phi(x) \phi^*(x) \right]. \quad (\text{C7})$$

Now we find from Eq. (C6)

$$\begin{aligned} \langle \phi(x) \phi^*(x') \rangle &= \langle \phi_1(x) \phi_1(x') + \phi_2(x) \phi_2(x') \rangle = \\ &\frac{1}{2} \delta(x-x') + \frac{1}{2} \delta(x-x') = \delta(x-x'), \end{aligned} \quad (\text{C8})$$

and

$$\begin{aligned} \langle \phi(x) \phi(x') \rangle &= \langle \phi_1(x) \phi_1(x') - \phi_2(x) \phi_2(x') + i\phi_1(x) \phi_2(x') + i\phi_2(x) \phi_1(x') \rangle = \\ &\frac{1}{2} \delta(x-x') - \frac{1}{2} \delta(x-x') = 0. \end{aligned} \quad (\text{C9})$$

Appendix D: Field theory without 1-clusters

An alternative way to formulate the clustering, without the use of clusters of size 1 is presented below. We shall show that a simple mapping reduces again to a special case of Eq. (6).

Consider a system in which we have only clusters of sizes a and b but no “inert” clusters of size 1. As explained in Section II the functional integration over the fields φ and φ^* requires matching each φ of a clustering center with a φ^* on the polymer, permitting no unmatched φ and φ^* pairs. Since size a and b clusters do not necessarily attach to each potential site on the polymer, all possible attachment sites have to be generated. The product

$$\prod_{i=1}^N (1 + \varphi^*(\mathbf{R}_i))$$

produces all equally weighted possibilities of the attaching to the sites $\{\mathbf{R}_i\}, \forall i \in \{1, \dots, N\}$ of a given polymer configuration.

The analog to Eq. (5) then becomes

$$\mathcal{Z}'_{N_a, N_b} = \mathcal{N} \int d\mathbf{R}_1 \dots d\mathbf{R}_N e^{-v \sum_{n,m=1}^N \delta(\mathbf{R}_n - \mathbf{R}_m)} \int [d\varphi][d\varphi^*] e^{-\int d\mathbf{r} \varphi(\mathbf{r}) \varphi^*(\mathbf{r})} \times \quad (\text{D1})$$

$$(1 + \varphi^*(\mathbf{R}_1)) G(\mathbf{R}_1, \mathbf{R}_2) (1 + \varphi^*(\mathbf{R}_2)) G(\mathbf{R}_2, \mathbf{R}_3) \dots G(\mathbf{R}_{N-1}, \mathbf{R}_N) (1 + \varphi^*(\mathbf{R}_N)) \times \frac{1}{N_a!} \left(\int d\mathbf{r} z_a \varphi^a(\mathbf{r}) \right)^{N_a} \frac{1}{N_b!} \left(\int d\mathbf{r} z_b \varphi^b(\mathbf{r}) \right)^{N_b}, \quad (\text{D2})$$

leading by the same procedure as described in Section II to analog of Eq. (6)

$$\begin{aligned} Z'_N &= \mathcal{N} \int [d\varphi][d\varphi^*] \left\{ \prod d\mathbf{R} \right\} \left\{ \prod G \right\} d^N \exp \left(- \int d\mathbf{r} \varphi(\mathbf{r}) \varphi^*(\mathbf{r}) + \right. \\ &\left. \int d\mathbf{r} \rho(\mathbf{r}) \ln(1 + \varphi^*(\mathbf{r})/d) + z_a \int d\mathbf{r} \varphi^a(\mathbf{r}) + z_b \int d\mathbf{r} \varphi^b(\mathbf{r}) \right). \end{aligned} \quad (\text{D3})$$

We see that the trivial transformation $\varphi^* \rightarrow \varphi^* - 1$ in Eq. (D3) above leads to the orginal field-theoretic equation in the main text, Eq. (6), with $z_1 \rightarrow 1$. For this reason we treat the marginally more general case in this paper.

Acknowledgments

R.F. gratefully acknowledges support from the NITheP of South Africa. K.K.M.-N. gratefully acknowledges the support of the National Research Foundation.

[1] R. S. Hoy and G. H. Fredrickson, J. Chem. Phys. **131**, 224902 (2009).

- [2] M. Rubinstein and A. V. Dobrynin, Current Opinion in Colloid & Interface Science **4**, 83 (1999).
- [3] A. N. Semenov and M. Rubinstein, Macromol. **31**, 1373 (1998).
- [4] M. Muthukumar, J. Chem. Phys. **104**, 691 (1996).
- [5] I. A. Nyrkova and A. N. Semenov, Eur. Phys. J. E **17**, 327 (2005).
- [6] R. T. Deam and S. F. Edwards, Phil. Trans. R. Soc. London A. Math. Phys. Sciences **280**, 317 (1976).
- [7] S. I. Kuchanov, S. V. Korolev, and S. V. Panyukov, Adv. Chem. Phys. **72**, 115 (1988).
- [8] A. V. Ermoshkin and I. Y. Erkhhimovich, J. Chem. Phys. **110**, 1781 (1999).
- [9] S. Kuchanov, H. Slot, and A. Stroeks, Prog. Polym. Sci. **29**, 563 (2004).
- [10] A. Kudlay and I. Y. Erkhhimovich, Macromol. Theory Simul. **10**, 542 (2001).
- [11] F. Sciortino, E. Bianchi, J. F. Douglas, and P. Tartaglia, J. Chem. Phys. **126**, 194903 (2007).
- [12] Yu. V. Kalyuzhnyi, C. -T. Lin, and G. Stell, J. Chem. Phys. **108**, 6525 (1998).
- [13] R. Nagarajan, J. Chem. Phys. **90**, 1980 (1989).
- [14] F. Ganazzoli, G. Raos, and G. Allegra, Macromol. Theory Simul. **8**, 65 (1999).
- [15] Tanaka, Macromolecules **23**, 3784 (1990).
- [16] B. Xu, A. Yekta, L. Li, Z. Masoumi, and M. A. Winnik, Colloid and Surfaces A **112**, 239 (1996).
- [17] A. N. Semenov, Macromol. **42**, 6761 (2009).
- [18] S. M. Loverde, A. V. Ermoshkin, and M. Olvera de la Cruz, J. Polym. Sci. Part B: Polym. Physics **43**, 796 (2005).
- [19] I. Y. Erkhhimovich and A. V. Ermoshkin, JETP **88**, 538 (1999).
- [20] F. Sciortino, A. Giacometti and G. Pastore, Phys. Rev. Lett. **103**, 237801 (2009).
- [21] Achille Giacometti, Fred Lado, Julio Largo, Giorgio Pastore, and Francesco Sciortino, J. Chem. Phys. **131**, 174114 (2009).
- [22] R. Fantoni , A. Giacometti, F. Sciortino, and G. Pastore, Soft Matter **7**, 2419 (2011).
- [23] S. F. Edwards, J. Phys. France **49**, 1673 (1988).
- [24] S. F. Edwards and K. F. Freed, J. Phys. C: Solid State Phys. **3**, 739 (1970).
- [25] S. F. Edwards and K. F. Freed, J. Phys. C: Solid State Phys. **3**, 750 (1970).
- [26] M. Gordon, Proc. R. Soc. Lond. A **268**, 240 (1962).
- [27] M. Gordon and G. R. Scantlebury, Trans. Faraday Soc. **60**, 604 (1964).
- [28] A. Mohan, R. Elliot, and G. H. Fredrickson, J. Chem. Phys. **133**, 174903 (2010).
- [29] Y. Bohbot-Raviv, T. M. Snyder, and Z.-G. Wang, Langmuir **20**, 7860 (2004).
- [30] M. E. Cates and T. A. Witten, Macromol. **19**, 732 (1986).
- [31] I. Nakamura and A.-C. Shi, J. Chem. Phys. **132**, 194103 (2010).
- [32] A. V. Ermoshkin and M. Olvera de la Cruz, J. Polym. Sc.: Part B: Polym. Phys. **42**, 766 (2004).
- [33] K. M. Hong and J. Noolandi, Macromolecules **14**, 727 (1981).
- [34] A. C. Shi, J. Noolandi, and R. C. Desai, Macromolecules **29**, 6487 (1996).
- [35] L. Leibler, Macromol. **13**, 1602 (1980).
- [36] V. N. Manoharan, M. T. Elsesser, and D. J. Pine, Science **301**, 483 (2003).
- [37] A. B. Pawar and I. Kretzschmar, Macromol. Rapid Commun. **31**, 150 (2010).
- [38] S. C. Glotzer and M. J. Solomon, Nature Materials **6**, 557 (2007).
- [39] Z. Zhang and S. C. Glotzer, Nano Letters **4**, 1407 (2004).
- [40] P. G. de Gennes, Rev. Mod. Phys. **64**, 645 (1992).
- [41] C. Casagrande, P. Fabre, M. Veyssié, and E. Raphaël, Europhys. Lett. **9**, 251 (1989).
- [42] L. Hong, A. Cacciuto, E. Luijten, and S. Granick, Nano Letters **6**, 2510 (2006).
- [43] A. Walther and A. H. Müller, Soft Matter **4**, 663 (2008).
- [44] Y. Ding, H. C. Öttinger, A. D. Schlüter, and M. Kröger, J. Chem. Phys. **127**, 094904 (2007).
- [45] J. U. Kim and M. W. Matsen, Phys. Rev. Lett. **102**, 078303 (2009).
- [46] P. Haronska and T. A. Vilgis, Phys. Rev. E **50**, 325 (1994).
- [47] T. A. Vilgis and P. Haronska, Macromol. **27**, 6465 (1994).
- [48] Notice that since the system has a finite volume V the Fourier transform are of the discrete type. In the thermodynamic limit $V \rightarrow \infty$ and $V^{-1} \sum_{\mathbf{k}} \dots \rightarrow \int d\mathbf{k}/(2\pi)^3 \dots$
- [49] K. K. Müller-Nedebock, S. F. Edwards, and T. C. B. McLeish, J. Chem. Phys. **111**, 8196 (1999).
- [50] M. Doi and S. F. Edwards, *The theory of polymer dynamics* (Clarendon Press, Oxford, 1986).
- [51] M. Doi, *Introduction to Polymer Physics* (Clarendon Press, Oxford, 1992).
- [52] T. Shimada, M. Doi, and K. Okano, J. Chem. Phys. **88**, 2815 (1988).
- [53] Note that for N_p polymer chains this expression should be modified as $\tilde{g}(k) = N_p/[\tilde{S}_0^{-1}(k)/V - 2CN_p]/\bar{\rho}$.

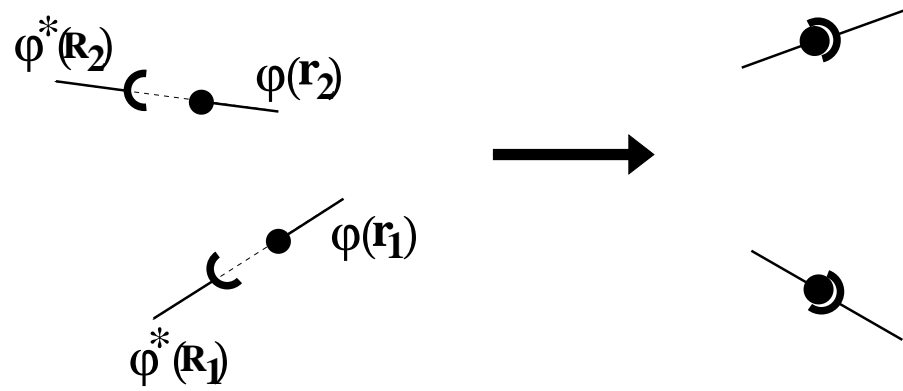


FIG. 1: A schematic representation of the role of the field-theory. The fields φ and φ^* are depicted as functions of spatial variables. Multiplication by $\exp(-\int \varphi\varphi^*)$ and subsequent functional integration enforces the linking of the spatial coordinates between pairs of φ and φ^* (in all possible ways).

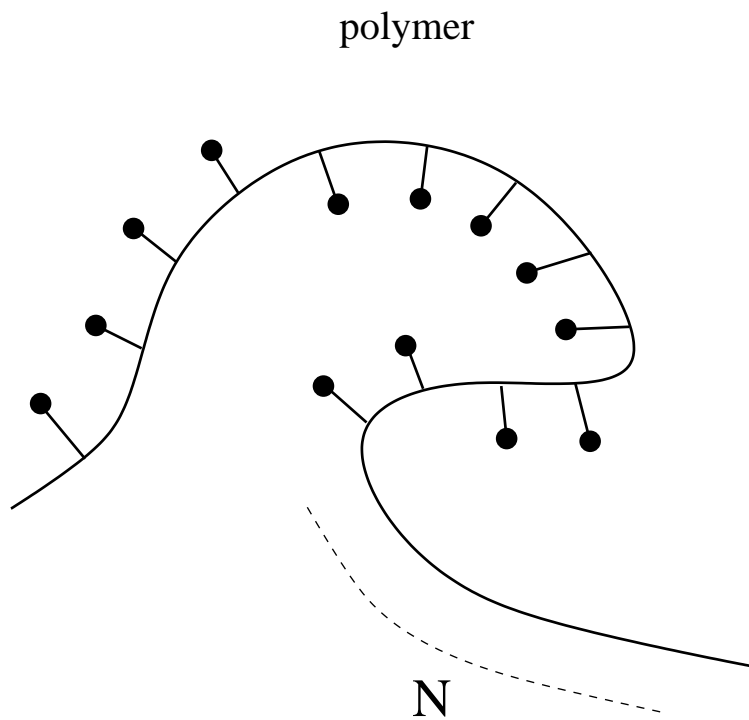


FIG. 2: Shows the polymer made up of N equispaced links that are susceptible to being linked into clusters.

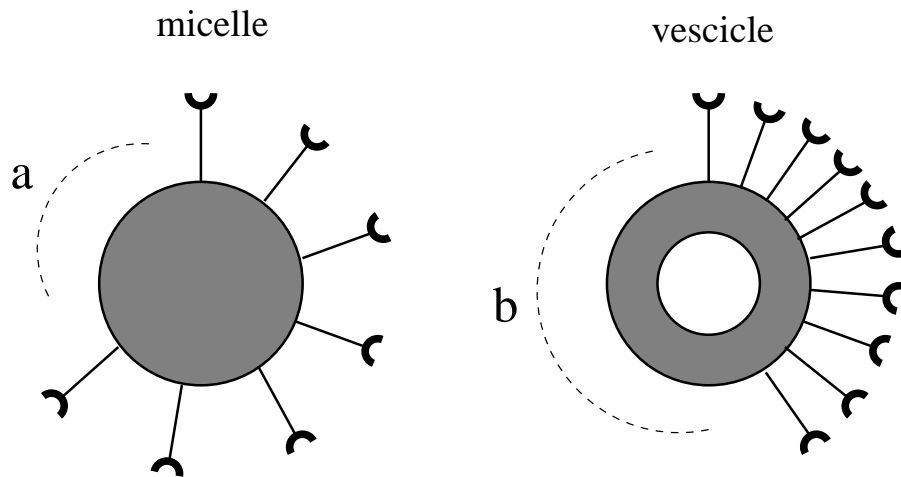


FIG. 3: Shows the clusters of Janus particles: the micelles are made of $a = 10$ links whereas the vesicles of $b = 40$ links.

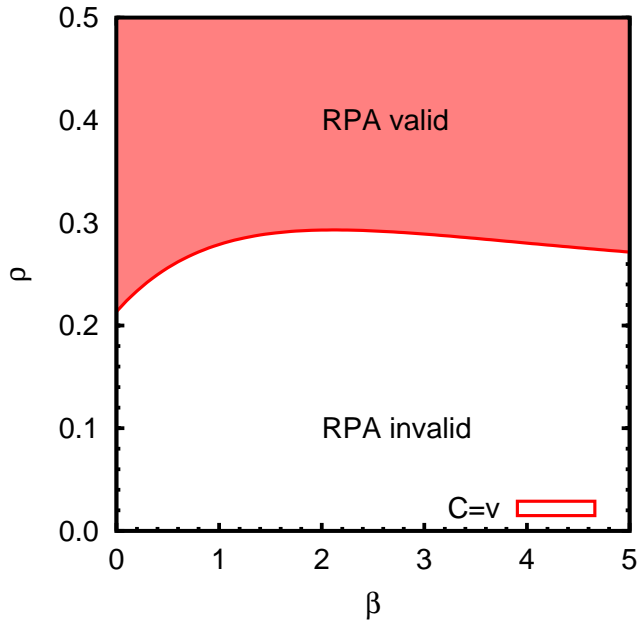


FIG. 4: (Color online) Shows the RPA validity region of the phase diagram, in the $a = 2, b = 0$ case, for $z_1 = 1, z_2 = e^{2\beta}$ and $v = 1$.

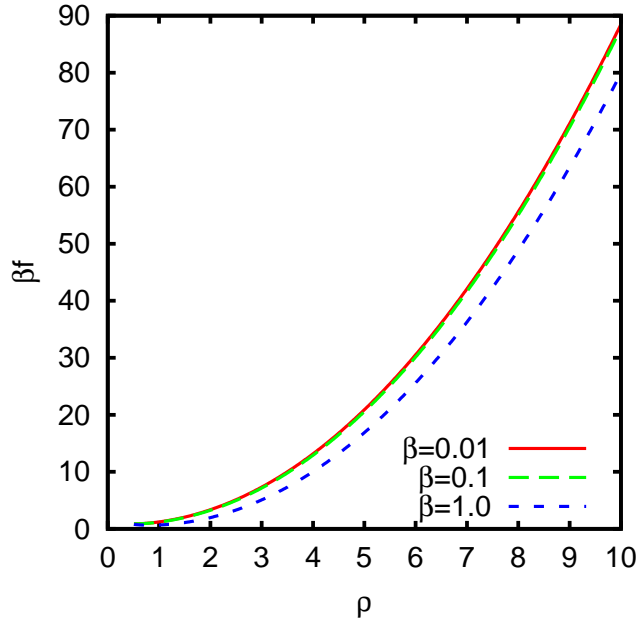


FIG. 5: (Color online) Shows the free energy density as a function of the average density in the $a = 2, b = 0$ case, for $z_1 = 1, z_2 = e^{2\beta}$ and $v = 1$.

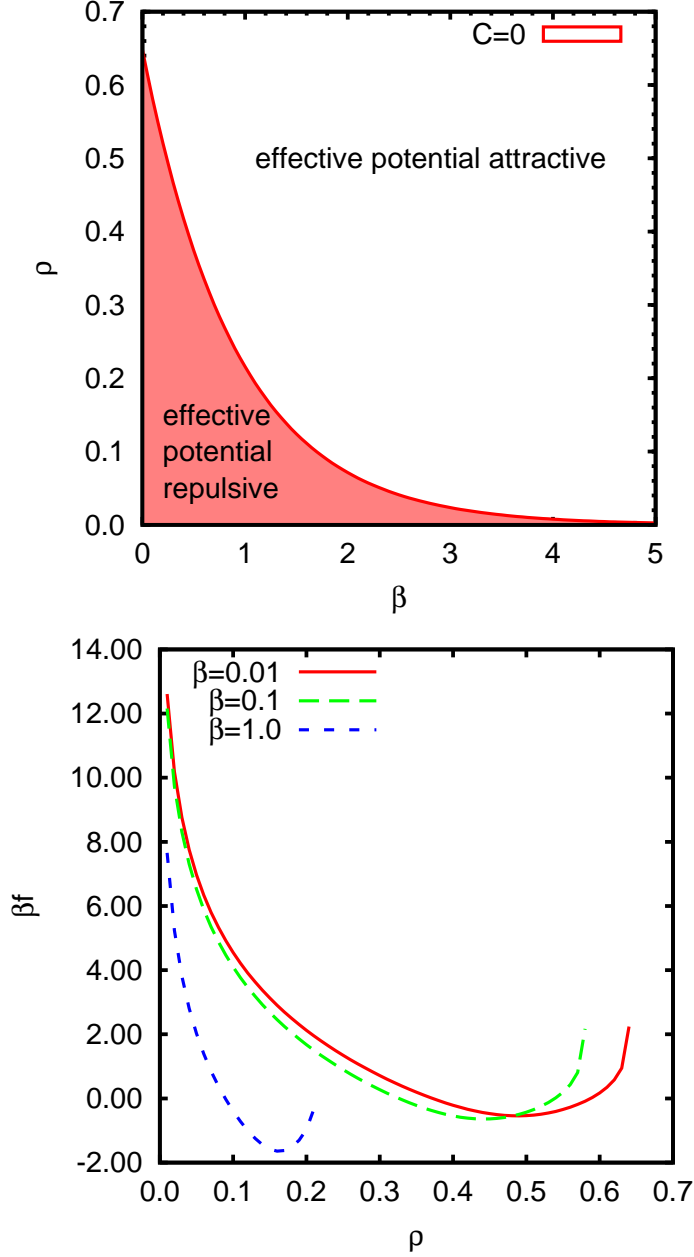


FIG. 6: (Color online) The upper panel shows the RPA validity region of the phase diagram, in the Janus case, for $z_1 = 1, z_{10} = e^{10\beta}, z_{40} = e^{40\beta}$, in the absence of any excluded volume effect. At $\beta = 0$ the $C = 0$ equation has solution $\rho \simeq 0.647933\dots$. Note that the validity region is in the small density region, where the contribution from the quadratic fluctuations of the theory dominates, and the whole theory is expected to be less significant. The lower panel shows the free energy density as a function of the average density. The rapid increase at high density is indicative of the limit of the RPA applicability.

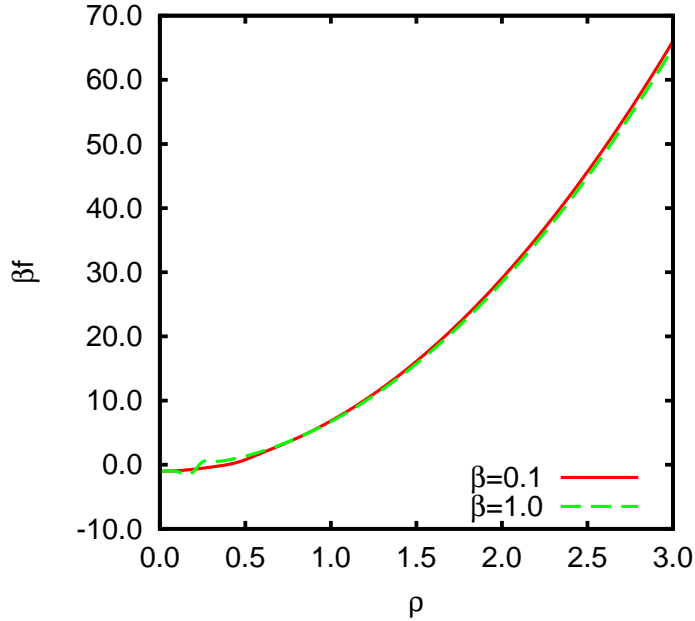


FIG. 7: (Color online) Shows the free energy density as a function of the average density in the Janus case, for $z_1 = 1$, $z_{10} = e^{10\beta}$, $z_{40} = e^{40\beta}$, and $v = 15$.

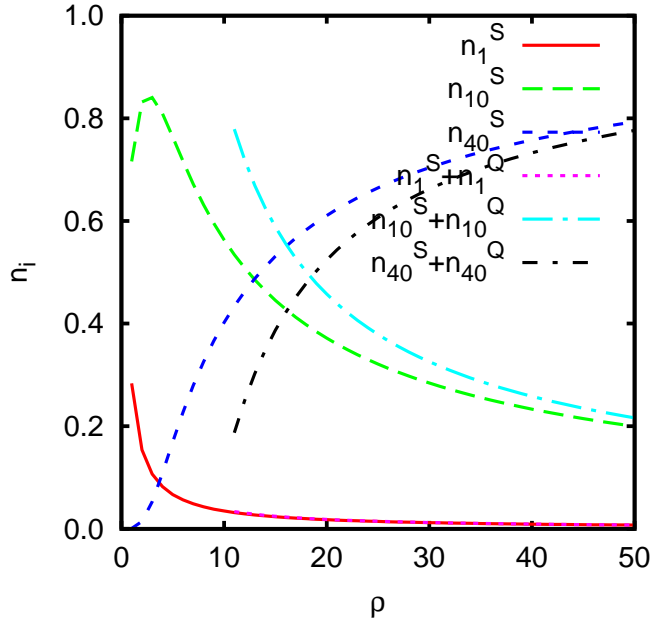


FIG. 8: (Color online) In the Janus case for $z_1 = 1, z_{10} = e^{10\beta}, z_{40} = e^{40\beta}, v = 15$, and $\beta = 1$ shows the concentrations of clusters of 1, 10, and 40 particles as a function of the density.

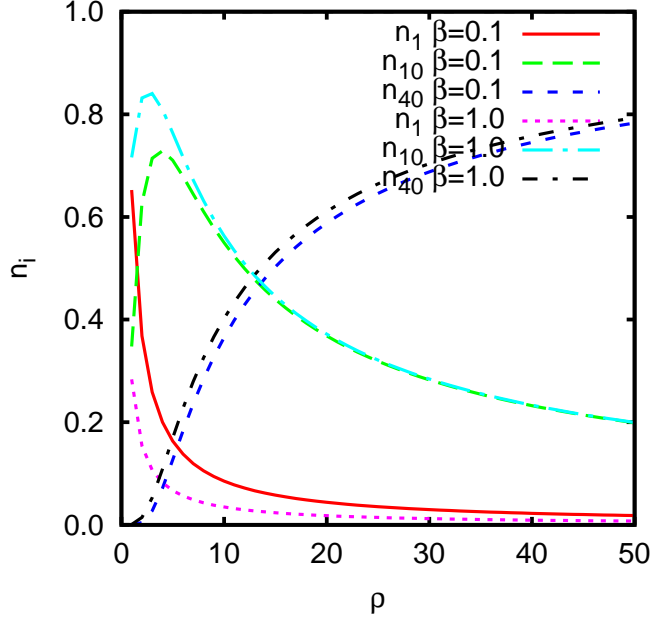


FIG. 9: (Color online) In the Janus case for $z_1 = 1, z_{10} = e^{10\beta}, z_{40} = e^{40\beta}$, and $v = 15$, shows the concentrations of clusters of 1 (n_1^S), 10 (n_{10}^S), and 40 (n_{40}^S) particles as a function of the density when we do not use the logarithmic correction in Eq. (24).

Figures captions

Figure 1: A schematic representation of the role of the field-theory. The fields φ and φ^* are depicted as functions of spatial variables. Multiplication by $\exp(-\int \varphi\varphi^*)$ and subsequent functional integration enforces the linking of the spatial coordinates between pairs of φ and φ^* (in all possible ways).

Figure 2: Shows the polymer made up of N equispaced links.

Figure 3: Shows the clusters of Janus particles: the micelles are made of $a = 10$ links whereas the vesicles of $b = 40$ links.

Figure 4: (Color online) Shows the RPA validity region of the phase diagram, in the $a = 2, b = 0$ case, for $z_1 = 1, z_2 = e^{2\beta}$ and $v = 1$.

Figure 5: (Color online) Shows the free energy density as a function of the average density in the $a = 2, b = 0$ case, for $z_1 = 1, z_2 = e^{2\beta}$ and $v = 1$.

Figure 6: (Color online) The upper panel shows the RPA validity region of the phase diagram, in the Janus case, for $z_1 = 1, z_{10} = e^{10\beta}, z_{40} = e^{40\beta}$, in the absence of any excluded volume effect. At $\beta = 0$ the $C = 0$ equation has solution $\rho \simeq 0.647933\dots$. Note that the validity region is in the small density region, where the contribution from the quadratic fluctuations of the theory dominates, and the whole theory is expected to be less significant. The lower panel shows the free energy density as a function of the average density. The rapid increase at high density is indicative of the limit of the RPA applicability.

Figure 7: (Color online) Shows the free energy density as a function of the average density in the Janus case, for $z_1 = 1, z_{10} = e^{10\beta}, z_{40} = e^{40\beta}$, and $v = 15$.

Figure 8: (Color online) In the Janus case for $z_1 = 1, z_{10} = e^{10\beta}, z_{40} = e^{40\beta}, v = 15$, and $\beta = 1$ shows the concentrations of clusters of 1, 10, and 40 particles as a function of the density.

Figure 9: (Color online) In the Janus case for $z_1 = 1, z_{10} = e^{10\beta}, z_{40} = e^{40\beta}$, and $v = 15$, shows the concentrations of clusters of 1 (n_1^S), 10 (n_{10}^S), and 40 (n_{40}^S) particles as a function of the density when we do not use the logarithmic correction in Eq. (24).